Super-Elastic Graphene Ripples for Flexible Strain Sensors

Yi Wang,[†,‡] Rong Yang,[†] Zhiwen Shi,[†,‡] Lianchang Zhang,[†] Dongxia Shi,[†] Enge Wang,[§] and Guangyu Zhang[†,*]

[†]Nanoscale Physics and Device Laboratory and [‡] Surface Physics Laboratory, Beijing National Laboratory for Condensed Matter Physics and Institute of Physics, Chinese Academy of Science, Beijing 100190, China, and [§]School of Physics, Peking University, Beijing 100871, China

ABSTRACT In this study, we report a buckling approach for graphene and graphene ribbons on stretchable elastomeric substrates. Stretched polydimethylsiloxane (PDMS) films with different prestrains were used to receive the transferred graphene, and nanoscale periodical buckling of graphene was spontaneously formed after strain release. The morphology and periodicity of the as-formed graphene ripples are dependent strongly on their original shapes and substrates' prestrains. Regular periodicity of the ripples preferred to form for narrow graphene ribbons, and both the amplitude and periodicity are reduced with the increase of prestrain on PDMS. The graphene ripples have the ability to afford large strain deformation, thus making it ideal for flexible electronic applications. It was demonstrated that both graphene ribbon and nanographene film ripples could be used for strain sensors, and their resistance changes upon different strains were studied. This simple and controllable process of buckled graphene provides a feasible fabrication for graphene flexible electronic devices and strain sensors due to its novel mechanical and electrical properties.

KEYWORDS: graphene · graphene ripples · mechanical buckling · flexible electronics · strain sensors

Since 2004, graphene has attracted tremendous attention because of its superior characteristics and potential applications.[1−3] Its two-dimensionality as well as its high flexibility, conductivity, and transparency make graphene a promising candidate for flexible electronics.[4−7] Usually, flat graphene sticks well to a flexible substrate, *e.g.*, polyethylene terephthalate or polydimethylsiloxane (PDMS), by weak van der Waals interaction. However, under a large structural deformation, sliding or even fracture is expected for graphene on its supporting substrate due to the rigid nature of graphene within its basal plane. A strategy for overcoming this adhesion failure under high levels of strain is to buckle graphene into 3D periodical structures, which can accommodate structural deformations as large as its supporting substrates.

Self-organized graphene ripples have been achieved for suspended or PMMA-supported graphene by heating,[4,5] but approaches of controllable graphene buckling on elastomeric substrates are still absent. In this article, we have fabricated buckled graphene on elastomeric PDMS substrate by using a nonlinear buckling technique, which was previously developed by Whitesides *et al.*[8] and widely applied for various materials.[9−16] Here we show the successful buckling of graphene on elastomeric PDMS substrate with nanoscale, periodic, ripple-like geometries. The as-made graphene ripples on PDMS show fully reversible structural deformations under large tensile strain (>30%), indicating their potential uses as flexible electronic materials under extreme stretching conditions. Strain sensors based on these buckled graphene ribbons or nanographene films on PDMS are demonstrated for detecting large levels of tensile strain.

RESULTS AND DISCUSSION

Fabrication of Graphene Ripples. The fabrication process is illustrated in Figure 1. An exfoliated graphene sample made by mechanical cleavage from HOPG was first put on SiO_2 (300 nm)/Si substrate with alignment marks. Graphene ribbon arrays were then fabricated by electron beam lithography and dry etching techniques as previously reported.[17] The graphene ribbons transfer process, from SiO_2/Si to prestrained PDMS, was carried out by following a recipe in which the PMMA thin film was used as mediator to manipulate graphene.[18,19] A ca. 300 nm thick PMMA (950 000 MW, 5 wt % in anisole) film was spin coated (at 4000 rpm) on SiO_2/Si substrate prior to the transfer, followed by baking at 170 °C for 2 h to obtain a thin film embedded with graphene ribbons. The PMMA/graphene ribbons film was then released from the SiO_2/Si substrate by wet chemical etching in aqueous KOH (1 mol, 80 °C) or HF (5%, 30 °C) solution. After a deionized water rinse, the released PMMA/graphene ribbons film was transferred and attached to a mechanically prestrained PDMS substrate with a thickness of ~2−4 mm. The tensile prestrain is defined as $\varepsilon = \Delta L/L$, where L is the PDMS initial length

* Address correspondence to gyzhang@aphy.iphy.ac.cn.

Received for review December 18, 2010 and accepted March 31, 2011.

Published online March 31, 2011
10.1021/nn103523t

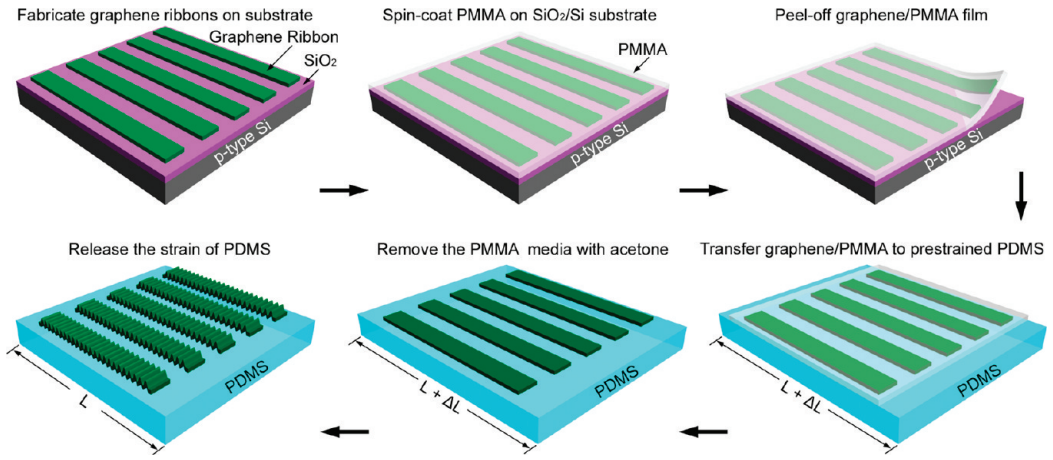

Figure 1. Schematic diagram of the process for buckled graphene ribbon fabrication on PDMS substrate. The graphene ribbon arrays on SiO_2(300 nm)/Si substrates are fabricated by electron beam lithography and dry etching, followed by 300 nm thick PMMA film spin coating and baking to obtain a thin film embedded with graphene ribbons. The PMMA/graphene ribbons film is then released from the SiO_2/Si substrate by wet chemical etching and then transferred and attached to a mechanically prestrained PDMS substrate with ribbon alignment along the prestrain direction. The buckled graphene ribbons are formed through releasing PDMS prestrain followed by removal of the PMMA overlay in hot acetone.

and ΔL is the relative length change after stretching. During the transfer process, these graphene ribbons were attached on the prestrained PDMS substrate with alignment along the strain direction. In order to remove the trapped water between PMMA/graphene and PDMS substrate, vacuum annealing at 100 °C for 30 min is necessary. The PMMA is finally removed in hot acetone (80 °C) before strain releasing. Releasing this prestrain of PDMS creates, through a nonlinear buckling process, graphene ripples with regular periodicities. This spontaneous formation of highly periodic and stretchable waved structures of graphene is well controlled by adjusting the ribbon geometry as well as the prestrain magnitude.

Figure 2a and b show AFM images of 500 nm wide monolayer graphene ribbon arrays before and after buckling. A 30% of prestrain was used for creating graphene ripples. The buckled narrow graphene ribbons all show very regular surface morphology with periodical structures, and the amplitude and periodicity of these graphene ripples are around ~80 and ~340 nm, correspondingly. The graphene ribbons tested for rippling usually have a length of 10 μm and width of up to 1−2 μm, and rippling can always be formed on the area covered with graphene through strain release. We also investigated the surface morphologies of monolayer graphene ripples formed under different prestrains. The left three images in Figure 3 (a, c, and e) show the AFM images of graphene ripples on PDMS formed under different prestrains of ε_{pre} = 10%, 20%, and 30%, respectively. The height profiles along the line cut marked in each image are shown to the right (Figure 3b, d, f), indicating the ripples' periodicities varying from 360 to 470 nm and amplitudes varying from 50 to 80 nm depending on different prestrains. It was noted that both the amplitudes and periodicities of the ripples decrease with increased prestrains. In addition, the ripple formation also depends on the width and thickness of the graphene ribbons: wider and thicker ribbons have larger amplitudes and periodicities, which is consistent with previous studies on other materials.[20−22]

Raman Spectroscopy Analysis. The spontaneous formation of graphene ripples during prestrain release results from the mismatch of the elastic modulus between graphene and the PDMS substrate. In addition to the geometry change, there is also compressive strain induced in the graphene basal plane after buckling. The strain can be detectable by Raman spectroscopy, as the D or 2D mode of graphene is very sensitive to strain,[23,24] where the D mode is the disorder-induced features associated with the double resonance scattering processes and the 2D mode is the second order of the D mode. The Raman spectra of a typical graphene sample before transfer (on SiO_2/Si, black curve) and after buckling (on PDMS, with prestrain of 30%, red curve) are shown in Figure 4. No obvious variations in either the G and D peak positions or the integrated intensity ratio of the 2D to G peak (I_{2D}/I_G) were observed even after many stretching-and-release cycles, indicating that the buckling process does not increase the defects of the graphene ribbons. However, the 2D peak of the graphene ripples on PDMS is blue-shifted by ~15 cm^{-1}, compared with the peak position for flat graphene on SiO_2/Si (~2700 cm^{-1}). Blue-shifts for both G and 2D peaks after annealing were found in the graphene ripples formed on PMMA,[5] while for our graphene ripples, the G peak shows no obvious change and only the 2D peak is blue-shifted. The G-peak line shift can be affected only by doping but not uniaxial strain.[23] As a result, the 2D peak shift is the optimal parameter for estimating uniaxial strain in

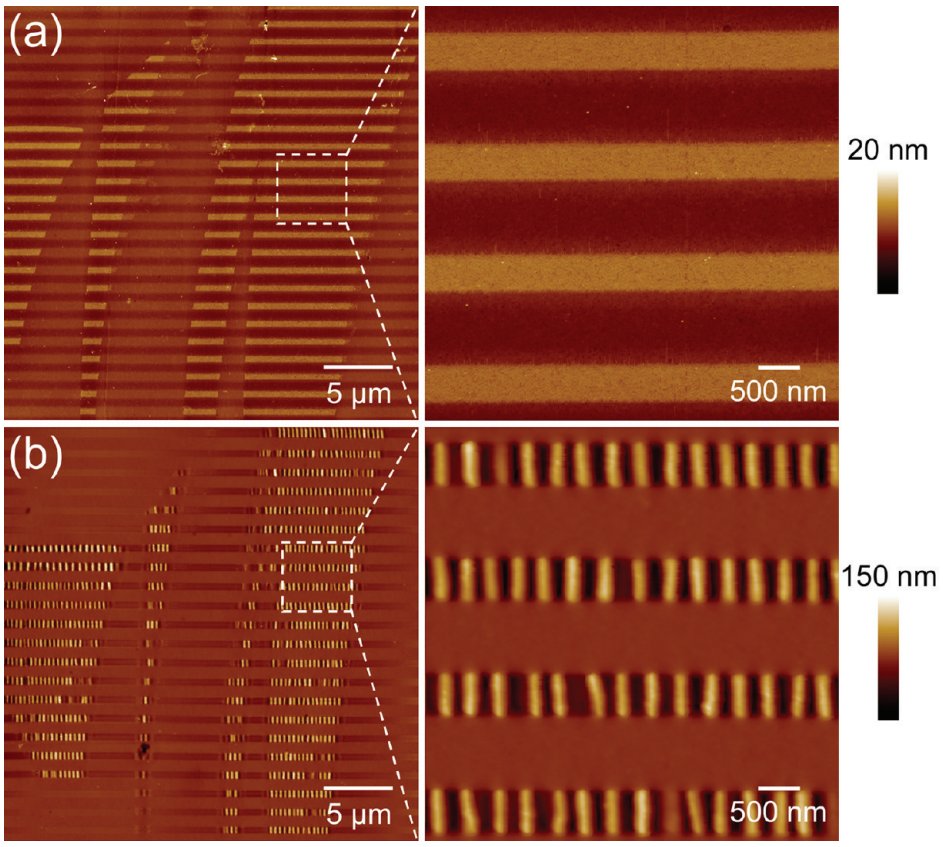

Figure 2. AFM images of graphene ribbon arrays before and after buckling. The prestrain on PDMS was 30% used to create graphene ripples. (a) Flat graphene ribbons before buckling, on SiO_2/Si substrate. (b) Buckled graphene ribbons after releasing prestrain on the PDMS substrate, showing periodic ripple shapes. Zoomed-in images for marked area of (a) and (b) are shown on the right.

Raman measurement. The blue-shift of the G peak in ref 5 might be caused by charge transfer doping after annealing. The blue-shift of the 2D peak is responsible for the compressive strain induced during the buckling process, and the amount of uniaxial strain in the graphene ripples can be roughly estimated from the formula $(\Delta\omega_{2D}/\varepsilon) = \omega_0\gamma_{2D}(1-0.186) \Rightarrow (\partial\omega_{2D}/\partial\varepsilon) \approx -64\ \mathrm{cm}^{-1}\%$.[25] The calculated Gruneisen parameter γ_{2D} is 2.84, as reported in ref 23. For the resulting $\Delta\omega_{2D}$ of 15 cm^{-1} in Figure 5d, the uniaxial strain is below 0.3%, which is quite small.

Two-Terminal Graphene Rippled Devices. Buckled graphene on flexible substrates can afford very high compressive and tensile strains, thus making it useful for high-level strain sensors. During stretching of the graphene ripples on PDMS, structural deformations can change the electrical conductivity, as graphene's electrical properties are very sensitive to its structural change. Two-terminal buckled graphene ribbon devices were fabricated on 300-nm-SiO_2/Si substrates with Ti (2 nm)/Au (50 nm) as the contact metals, then transferred to prestrained PDMS. The contact electrodes were defined by electron beam lithography, metal deposition, and lifting-off techniques prior to graphene transfer. After prestrain releasing, graphene ripples between the source and drain electrodes were created. Note that the buckling for electrodes was also created but with much larger periodicity (around 10 μm scale for 5 μm wide electrodes; refer to inset in Figure 5a). *I*–*V* curves of a device under different tensile strains of the device on PDMS (Figure 5a) show several important features, which are further developed in the plots shown in Figure5b. For this particular device, graphene ripples were formed with a PDMS prestrain of 20% from a graphene ribbon with an original width of 1.5 μm and length of 22.8 μm. From the data, we can see that the linear *I*–*V* characteristics are inherent not only for flat graphene but also for buckled graphene, indicating their metallic nature. Figure 5b shows the device resistance response upon different tensile strains. The device resistance decreases linearly from 5.9 to 3.6 kΩ when experiencing a strain of 0% to 20%. The minimum resistance of 3.6 kΩ corresponds to a state of totally relaxed graphene, that is, flat graphene. Compared with the flat graphene, the resistance increase of the graphene ripples can be ascribed to the nonflatness for buckled geometries, since the effective length of graphene ripples stay the same during buckling. Note that the intrinsic strain induced by buckling in these graphene ripples is very small (less than 0.3%, as mentioned above), and the resistance change due to the intrinsic strain is insignificant. Graphene's nonflatness can act as an additional source of scattering for charge carriers, thus leading

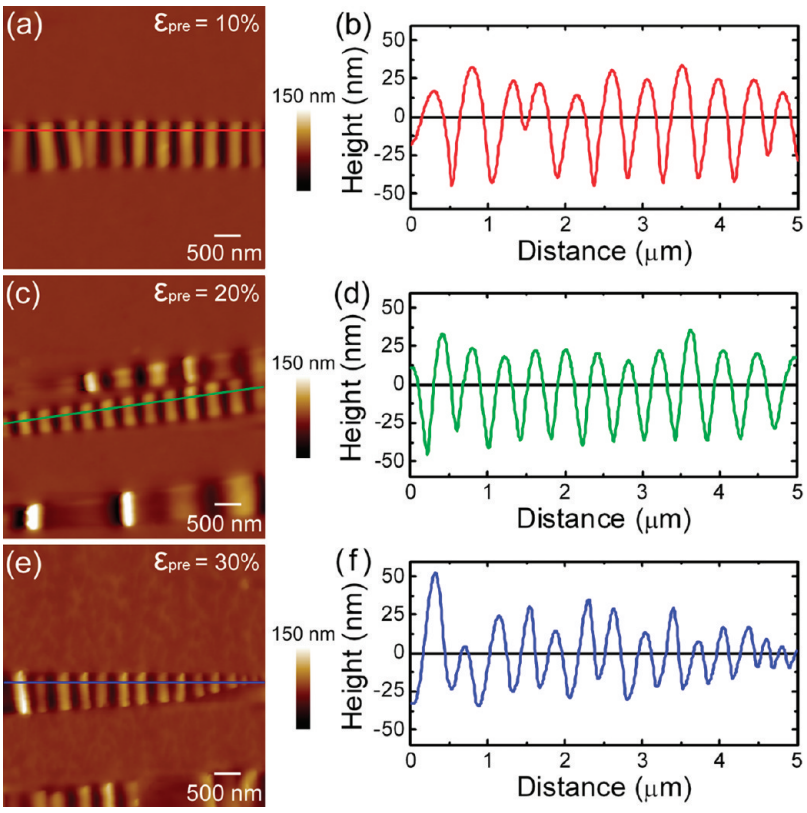

Figure 3. Monolayer graphene ripples formed under different prestrains on PDMS. (a, c, and e) AFM images of graphene ripples formed under prestrains of ε_{pre} = 10%, 20%, and 30%, respectively. (b, d, and f) Height profiles along the line marked in (a), (c), and (e), respectively.

to increased resistance.[26] Our results are also consistent with the experimental observations reported in the ref 27. The gauge factor (GF) is defined by the ratio of relative change in electrical resistance to the mechanical strain, and GF ≈ -2 was derived for this device from the plots.

We also fabricated a buckled nanographene film on PDMS by a similar technique to that described above. The film consists of uniform nanographene domains (with domain size of tens of nanometers) connecting with each other by stacking overlaps at the edges,[28] and the AFM image of the film after buckling (PDMS prestrain ε_{pre} = 30%) is shown in Figure 5c. Sheet resistance of the buckled nanographene film under different tensile strains was measured with a GF $\approx$ 0.55 (Figure 5d), showing an opposite trend of that shown in Figure 5b. The sheet resistance of the nanographene network mainly comes from the interconnections of adjacent nanographene domains. After buckling, these nanographene domains become more compact and overlapped for the interconnections, leading to reduced electrical percolation pathways in the film. Thus, the increased sheet resistance of the buckled nanographene film was achieved during the flattening/stretching process. It is noted that the process of buckling and stretching either in buckled graphene ribbons or in nanographene films is fully reversible, and the electrical and mechanical relation is stable in each buckling and stretching cycle.

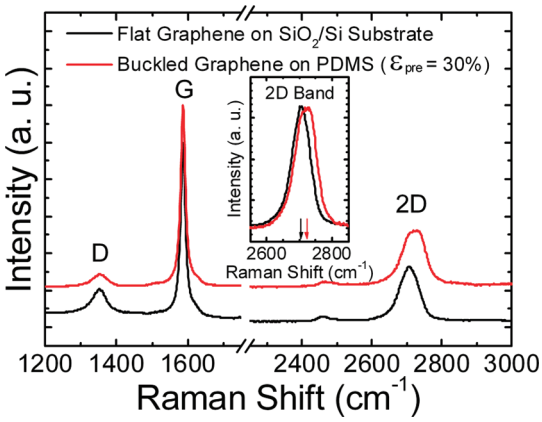

Figure 4. Typical Raman spectra of graphene before buckling on SiO_2/Si (black curve) and after buckling on PDMS (red curve) in the same region. The vertical arrows in the inset indicate the expected 2D band position (~2700 cm^{-1}) change. For the spectra marked with red, the PDMS substrate Raman signal was already subtracted.

CONCLUSIONS

In summary, two-dimensional structures of graphene can be integrated with a prestrained elastomeric substrate to create buckled layouts. The results presented here are the first observations of nonlinear buckling morphology in graphene ribbons. The geometrical configurations of these graphene ribbons depend on the prestrains of the elastomeric substrates

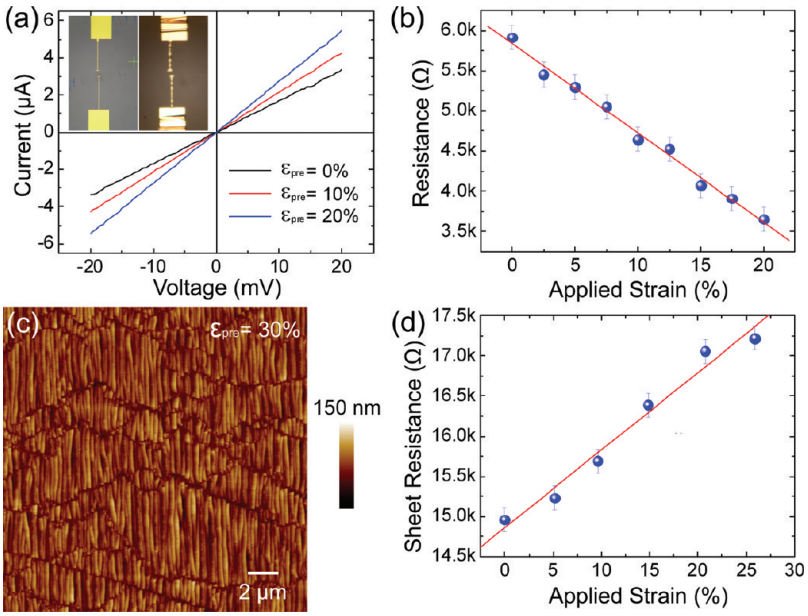

Figure 5. Comparison of resistance response under different strain between the rippled graphene device and buckled nanographene film device. (a) *I*−*V* curves of a two-terminal ripple graphene device under different strain. The insets are optical images before and after buckling. 20% prestrain was used to create the rippled graphene device. The width and length of the conducting graphene ribbon prior to buckling are 1.5 and 22.8 μm, respectively. (b) Resistance response of the rippled graphene device upon different strain. The resistance decreases linearly from 5.9 to 3.6 kΩ when experiencing a strain of 0% to 20%. The minimum resistance of 3.6 kΩ corresponds to a state of totally relaxed flat graphene. (c) AFM image of a buckled nanographene film for a sample prepared with ε_{pre} = 30%. (d) Resistance of the buckled nanographene film device as a function of applied strain, which shows a trend opposite of rippled graphene in (b).

used in the fabrication and also on the width and thickness of graphene. The resistance characteristics of buckled graphene ribbons and nanographene films in the buckling and stretching process demonstrate the capabilities of graphene in high-performance strain sensor applications. Our precise and controllable fabrication of buckled graphene ribbons and nanographene films provides an easy and feasible method for a scaled-up process of buckled graphene for potential flexible electronic devices.

METHODS

Sample Preparation and Lithographic Patterning. Graphene samples were prepared by mechanical cleavage method from HOPG (grades ZYA from SPI) and transferred to the 300-nm-SiO_2/P^{+2}-Si substrate. The SiO_2 substrates were premarked for both sample and lithography positioning. Five percent PMMA in anisole was spin-coated at 4000 rpm on the as-prepared samples, and e-beam lithography (Raith 150 system) and oxygen plasma etching were used for patterning of graphene into various ribbon arrays. Oxygen plasma etching was performed in a reactive ion etching system (PlasmaLab 80 Plus, Oxford Instruments Company) by using pure O_2 as reactive gas, 100 W of plasma power, and 0.1 Torr of pressure for 10 s.

AFM and Raman Characterization. The surface morphologies of the as-made graphene ripples were investigated by atomic force microscopy (AFM) in the tapping mode (Veeco Instrument, multimode, NanoScope IIId). All the Raman spectra were measured by a Jobin Yvon T64000 system. The excitation light is a 532 nm laser, with an estimated laser spot size of 1 μm. To avoid damaging and heating, the laser power was controlled at 1 mW.

Device Fabrication and Measurements. Graphene ribbons patterned on 300-nm-thick SiO_2 on Si substrate were used for device fabrication by e-beam lithography, metal deposition (Ti (1.5 nm)/Au (30 nm), by e-beam evaporation), and lifting-off techniques. Then the two terminal graphene ribbon devices were transferred from the SiO_2/Si substrate to prestrained PDMS using the same transfer processing for graphene. After removing the PMMA overlay and prestrain releasing, the rippled graphene device was achieved. Electrical properties were characterized in air with an Agilent semiconductor parameter analyzer (4156C).

Acknowledgment. This work was supported by the Institute of Physics (IOP) start-up funding, 100 Talents Program of the Chinese Academy of Sciences (CAS), National 973 project of China (grant no. 2010CB934202), and Science Foundation of CAS and the National Science Foundation of China (NSFC, grant nos. 11074288 and 10974226).

Supporting Information Available: Additional details regarding experimental tools, atomic force microscopy measurement details, Raman characteristics details, device fabrication and measurements details, and electrical measurement of graphene films are included. This material is available free of charge *via* the Internet at http://pubs.acs.org.

REFERENCES AND NOTES

1. Pereira, V. M.; Neto, A. H. C. Strain Engineering of Graphene's Electronic Structure. *Phys. Rev. Lett.* **2009,** *103*, 046801-1–046801-4.
2. Katsnelson, M. I.; Geim, A. K. Electron Scattering on Microscopic Corrugations in Graphene. *Phil. Trans. R. Soc. A* **2008,** *366*, 195–204.
3. Guinea, F.; Katsnelson, M. I.; Vozmediano, M. A. H. Midgap States and Charge Inhomogeneities in Corrugated Graphene. *Phys. Rev. B* **2008,** *77*, 075422-1–075422-8.

4. Bao, W. Z.; Miao, F.; Chen, Z.; Zhang, H.; Jang, W. Y.; Dames, C.; Lau, C. N. Controlled Ripple Texturing of Suspended Grapheme and Ultrathin Graphite Membranes. *Nat. Nanotechnol.* **2009,** *4*, 562–566.
5. Li, Z. J.; Cheng, Z. G.; Wang, R.; Li, Q.; Fang, Y. Observation of Graphene Bubbles and Effective Mass Transport under Graphene Films. *Nano Lett.* **2009,** *9*, 3599–3602.
6. Yu, T.; Ni, Z. H.; Du, C. L.; You, Y. M.; Wang, Y. Y.; Shen, Z. X. Raman Mapping Investigation of Graphene on Transparent Flexible Substrate: The Strain Effect. *J. Phys. Chem. C* **2008,** *112*, 12602–12605.
7. Zhang, J.; Xiao, J. L.; Meng, X. H.; Monroe, C.; Huang, Y. G.; Zou, J.-M. Free Folding of Suspended Graphene Sheets by Random Mechanical Stimulation. *Phys. Rev. Lett.* **2010,** *104*, 166805-1–166805-4.
8. Bowden, N.; Brittain, S.; Evans, A. G.; Hutchinson, J. W.; Whitesides, G. M. Spontaneous Formation of Ordered Structures in Thin Films of Metals Supported on an Elastomeric Polymer. *Nature* **1998,** *393*, 146–149.
9. Baca, A. J.; Ahn, J.-H.; Sun, Y.; Meitl, M. A.; Menard, E.; Kim, H.-S.; Choi, W. M.; Kim, D.-H.; Huang, Y.; Rogers, J. A. Semiconductor Wires and Ribbons for High-Performance Flexible Electronics. *Angew. Chem., Int. Ed.* **2008,** *47*, 5524–5542.
10. Ryu, S. Y.; Xiao, J.; Park, W. I.; Son, K. S.; Huang, Y. Y.; Paik, U.; Rogers, J. A. Lateral Buckling Mechanics in Silicon Nanowires on Elastomeric Substrates. *Nano Lett.* **2009,** *9*, 3214–3219.
11. Schmidt, O. G.; Eberl, K. Nanotechnology: Thin Solid Films Roll Up into Nanotubes. *Nature* **2001,** *410*, 168.
12. Zhang, L.; Ruh, E.; Grützmacher, D.; Dong, L.; Bell, D. J.; Nelson, B. J.; Schnenberger, C. Fabrication and Characterization of Three-Dimensional InGaAs/GaAs Nanosprings. *Nano Lett.* **2006,** *6*, 1311–1317.
13. Sun, Y.; Choi, W. M.; Jiang, H.; Huang, Y. Y.; Rogers, J. A. Controlled Buckling of Semiconductor Nanoribbons for Stretchable Electronics. *Nat. Nanotechnol.* **2006,** *1*, 201–207.
14. Sun, Y.; Kumar, V.; Adesida, I.; Rogers, J. A. Buckled and Wavy Ribbons of GaAs for High-Performance Electronics on Elastomeric Substrates. *Adv. Mater.* **2006,** *18*, 2857–2862.
15. Khang, D.; Jiang, H.; Huang, Y.; Rogers, J. A. A Stretchable Form of Single-Crystal Silicon for High-Performance Electronics on Rubber Substrates. *Science* **2006,** *311*, 208–212.
16. Khang, D.-Y.; Xiao, J.; Kocabas, C.; MacLaren, S.; Banks, T.; Jiang, H.; Huang, Y. Y.; Roger, J. A. Molecular Scale Buckling Mechanics in Individual Aligned Single-Wall Carbon Nanotubes on Elastomeric Substrates. *Nano Lett.* **2008,** *8*, 124–130.
17. Yang, R.; Zhang, L. C.; Wang, Y.; Shi, Z. W.; Shi, D. X.; Gao, H. J.; Wang, E. G.; Zhang, G. Y. An Anisotropic Etching Effect in the Graphene Basal Plane. *Adv. Mater.* **2010,** *22*, 4014–4019.
18. Jiao, L. Y.; Fan, B.; Xian, X. J.; Wu, Z. Y.; Zhang, J.; Liu, Z. F. Creation of Nanostructures with Poly(methyl methacrylate-)-Mediated Nanotransfer Printing. *J. Am. Chem. Soc.* **2008,** *130*, 12612–12613.
19. Reina, A.; Son, H. B.; Jiao, L. Y.; Fan, B.; Dresselhaus, M. S.; Liu, Z. F.; Kong, J. Transferring and Identification of Single- and Few-Layer Graphene on Arbitrary Substrates. *J. Phys. Chem. C* **2008,** *112*, 17741–17744.
20. Jiang, H. Q.; Khang, D.-Y.; Song, J. Z.; Sun, Y. G.; Huang, Y. G.; Rogers, J. A. Finite Deformation Mechanics in Buckled Thin Films on Compliant Supports. *Proc. Natl. Acad. Sci. U. S. A.* **2007,** *104*, 15607–15612.
21. Jiang, H. Q.; Khang, D.-Y.; Fei, H. Y.; Kim, H.; Huang, Y. G.; Xiao, J. L.; Rogers, J. A. Finite Width Effect of Thin Films Buckling on Compliant Substrate: Experimental and Theoretical Studies. *J. Mech. Phys. Solids* **2008,** *56*, 2585–2598.
22. Khang, D.-Y.; Rogers, J. A.; Lee, H. H. Mechanical Buckling: Mechanics, Metrology, and Stretchable Electronics. *Adv. Funct. Mater.* **2008,** *19*, 1526–1536.
23. Mohiuddin, T. M. G.; Lombardo, A.; Nair, R. R.; Bonetti, A.; Savini, G.; Jalil, A.; Bonini, N.; Basko, D. M.; Galiotis, C.; Marzari, N.; *et al*. Uniaxial Strain in Graphene by Raman Spectroscopy: G Peak Splitting, Grüneisen Parameters, and Sample Orientation. *Phys. Rev. B* **2009,** *79*, 205433-1–205433-8.
24. Ferrari, A. C.; Meyer, J. C.; Scardaci, V.; Casiraghi, C.; Lazzeri, M.; Mauri, F.; Piscanec, S.; Jiang, D.; Novoselov, K. S.; Roth, S.; *et al*. Raman Spectrum of Graphene and Graphene Layers. *Phys. Rev. Lett.* **2006,** *97*, 187401-1–187401-4.
25. Thomsen, C.; Reich, S.; Ordejón, P. Ab initio Determination of the Phonon Deformation Potentials of Graphene. *Phys. Rev. B* **2002,** *65*, 073403-1–073403-3.
26. Katsnelson, M. I.; Geim, A. K. Electron Scattering on Microscopic Corrugations in Graphene. *Phil. Trans. R. Soc. A* **2008,** *366*, 195–204.
27. Kim, K. S.; Zhao, Y.; Jang, H.; Lee, S. Y.; Kim, J. M.; Kim, K. S.; Ahn, J. H.; Kim, P.; Choi, J. Y.; Hong, B. H. Large-scale Pattern Growth of Graphene Films for Stretchable Transparent Electrodes. *Nature* **2009,** *457*, 706–710.
28. Zhang, L, C.; Shi, Z. W.; Wang, Y.; Yang, R.; Shi, D. X.; Zhang, G. Y. Catalyst-free Growth of Nanographene Film on Various Substrates. *Nano Res.* **2011,** *4*, 315–341.